CrystEngComm

COMMUNICATION

View Article Online
View Journal | View Issue

Cite this: *CrystEngComm*, 2017, **19**, 4704

Received 8th June 2017,
Accepted 20th July 2017

DOI: 10.1039/c7ce01077j

rsc.li/crystengcomm

Molecular recognition and solvatomorphism of a cyclic peptoid: formation of a stable 1D porous framework†

Eleonora Macedi,[a] Alessandra Meli,[a] Francesco De Riccardis,[a] Patrizia Rossi,[b] Vincent J. Smith,[c] Leonard J. Barbour,[c] Irene Izzo*[a] and Consiglia Tedesco*[a]

Molecular recognition and the hydrophobic effect explain the solvatomorphic behavior of a hexameric α-cyclic peptoid. Either a pure non-porous crystal form or a stable one-dimensional porous framework is obtained using an appropriate choice of crystallization solvents.

The study of molecular aggregation in solution to form crystalline solids represents the focus of interdisciplinary research efforts.[1,2] Understanding of the supramolecular aspects in the nucleation step is crucial to controlling the overall outcome of the crystallization process. A holistic approach takes into account both the structural diversity and the possible interaction patterns of the involved species to exploit the chemistry of nucleation.[3] In particular, a recent total scattering study demonstrated that solvent molecules restructure around the forming nanoparticles depending on the nature of their counterparts.[4] Thus, the solvent plays a key role in determining the resulting crystal form.[5] Conformational flexibility adds further complexity to the crystallization process, giving rise to conformational polymorphs that differ not only in the packing mode, but also in the molecular conformation.[6]

In our ongoing studies on cyclic peptoids,[7–10] we have investigated the role of the crystallization solvent in the solid state assembly of the cyclic hexamer cyclo-(Nme-Npa$_2$)$_2$ (compound **1** in Scheme 1, Nme = *N*-(methoxyethyl)glycine, Npa = *N*-(propargyl)glycine) and reported its peculiar solid state dynamics.[11] Compound **1** crystallizes from acetonitrile as form **1A** and undergoes a reversible single-crystal-to-single-crystal transformation upon the release of guest molecules with a drastic conformational change to give the desolvated crystal form **1B**.[11] In form **1A**, methoxyethyl and propargyl side chains extend vertically with respect to the macrocycle plane, inducing the columnar arrangement of peptoid macrocycles. Upon acetonitrile removal, two vertical propargyl side chains tilt by 113° and form an unprecedented CH–pi zipper that links together the peptoid columns in the desolvated crystal form **1B**. Thereafter, upon the exposure to acetonitrile molecules, the CH–pi zipper opens up and transforms back to the solvated form **1A**.[11]

Subsequent to these intriguing results, we report herein a polymorph screening of compound **1** with a view to understanding the role of the crystallization solvent on the solid state assembly (Scheme 1). In particular, we obtained and characterized two new crystal forms of **1**, namely **1C** and **1D**. We were also able to derive two other crystal forms **1E** and **1F** from **1D**, with **1F** being a stable empty porous form.

1C and **1D** were crystallized by slow evaporation from acetonitrile/water and acetonitrile/methanol solutions, respectively (Scheme 1, see the ESI† for further details).

Single crystal X-ray diffraction (see Table 1 and also Fig. S1–S3, ESI†) showed that **1C** crystallizes as a pure form, whereas **1D** is a methanol solvate. In both crystal forms, the macrocycle possesses a crystallographic inversion centre and exhibits a distorted *cctcct* peptoid backbone conformation (where *c* denotes *cis* and *t* denotes *trans*).[12]

Nevertheless, the macrocycle conformation in **1C** and **1D** is remarkably different from each other: in **1C**, two propargyl residues feature a *trans* conformation, while in **1D** the methoxyethyl residues correspond to the *trans* residues, as observed in crystal forms **1A** and **1B** (Fig. 1 and S4–S6, ESI†).[11]

Gas phase energy optimization[13] indicates that the novel molecular conformation observed in crystal form **1C** is less stable by 30 kJ mol^{-1} with respect to that observed in **1D** (see the ESI† for details).

Hirshfeld surface analysis[14] and lattice energy calculations using the PIXEL method[15] allowed us to quantitatively assess

[a] *Department of Chemistry and Biology "A. Zambelli", University of Salerno, Via Giovanni Paolo II 132, 84084 Fisciano (SA), Italy. E-mail: ctedesco@unisa.it*
[b] *Department of Industrial Engineering, University of Florence, via S. Marta 3, I-50139 Florence, Italy*
[c] *Department of Chemistry and Polymer Science, University of Stellenbosch, Private Bag X1, 7602 Matieland, Stellenbosch, South Africa*

† Electronic supplementary information (ESI) available. CCDC 1545931–1545934. For ESI and crystallographic data in CIF or other electronic format see DOI: 10.1039/c7ce01077j

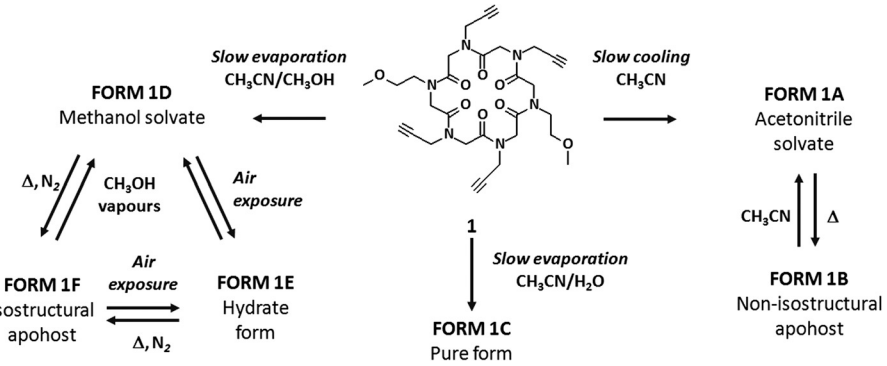

Scheme 1 Crystal forms of cyclo-(Nme-Npa$_2$)$_2$ **1**, where Nme = *N*-(methoxyethyl)glycine and Npa = *N*-(propargyl)glycine.

the main assembly motifs in the two crystal forms (Fig. 1 and S7–S9 and Tables S2 and S3, ESI†).

In **1C**, a layered arrangement in the *ab* plane is provided by backbone-to-side chain CO···H$_2$C interactions involving the *cis* carbonyl groups and both propargyl residues (Fig. 1C, S7c and S8 and motifs I and II in Table S1, ESI†). In **1D**, a columnar arrangement along the shortest axis is provided by backbone-to-side chain CO···HC≡C interactions involving the *trans* carbonyl groups and the vertical *cis* propargyl side chains (Fig. 1D, S7d and S9 and motif I in Table S2, ESI†). Vertical propargyl side chains act as pillars and extend vertically with respect to the macrocycle plane interacting with the backbone atoms of the macrocycles below and above, as previously observed.[8,9,10a,11]

In **1C**, layers are interconnected along the *c* axis by the backbone-to-side chain interactions by means of C=O···H–C≡C and pi–pi interactions involving the *cis* propargyl side chains (Fig. S8 and motifs III and IV in Table S1†). In **1D**, intercolumnar interactions are provided by backbone-to-side chain C=O···H–C≡C interactions and involve the horizontal propargyl side chains (Fig. S9 and motif II in Table S2, ESI†).

Thus, we obtained two different molecular conformations in crystal forms **1C** and **1D** by changing the molecular environment during the crystallization process. In particular, adding water to the crystallization solvent triggers a new conformation induced by a hydrophobic effect. In **1C**, the more hydrophilic methoxyethyl side chains are oriented horizontally with respect to the macrocycle plane and are more exposed with respect to **1D**, where the methoxyethyl side chains are vertical and eventually embedded in the cyclopeptoid columns (Fig. 1 and S7c and d, ESI†). Moreover, the layered assembly in **1C** allows the maximization of the interactions among the hydrophobic propargyl side chains.

Adding methanol to the acetonitrile solution does not have the same conformational effect observed in **1C**; indeed, its molecular conformation is the same as that obtained in **1A** using only acetonitrile as the crystallization solvent.[16]

Methanol molecules in form **1D** occupy cavities between the columns (with a volume of 84.4 Å^3 per unit cell,[17] Fig. 2 and 3b), and are hydrogen bonded to the *cis* carbonyl oxygen atoms O2 (CO···HO 1.79 Å, CO···HO 173°). The carbonyl oxygen atoms O2 act as H-bond binding sites (Fig. S7d, ESI†).

Table 1 Crystallographic data for **1C**, **1D**, **1E** and **1F**

	1C	**1D**	**1E**	**1F**
T	296 K	100 K	100 K	100 K
Formula	$C_{30}H_{38}N_6O_8$	$C_{30}H_{38}N_6O_8{\cdot}2CH_3OH$	$C_{30}H_{38}N_6O_8{\cdot}1.16H_2O$	$C_{30}H_{38}N_6O_8$
Formula weight	610.66	667.06	628.68	610.66
System	Triclinic	Triclinic	Triclinic	Triclinic
Space group	$P\bar{1}$	$P\bar{1}$	$P\bar{1}$	$P\bar{1}$
a (Å)	8.814(3)	8.5007(14)	8.5852(15)	8.5875(8)
b (Å)	9.0944(18)	10.3965(11)	10.4929(17)	10.3508(8)
c (Å)	10.982(4)	10.9102(17)	10.556(2)	10.6762(8)
α (°)	78.86(2)	67.863(11)	68.110(9)	67.884(7)
β (°)	87.55(3)	84.552(15)	86.318(10)	86.630(7)
γ (°)	66.35(2)	71.048(13)	67.035(9)	68.351(8)
V (Å^3)	790.6(4)	844.3(2)	808.8(3)	813.60(13)
Z	1	1	1	1
D_X (g cm^{-3})	1.283	1.327	1.297	1.246
μ (mm^{-1})	0.094	0.099	0.097	0.092
F_{000}	324.0	360.0	336.0	324.0
R ($I > 2\sigma I$)	0.0762(1454)	0.0700(2055)	0.0582(1780)	0.0492(2051)
wR_2 (all)	0.2567(3541)	0.1966(3798)	0.1560(3240)	0.1099(3081)
N. param.	200	218	212	199
GooF	0.986	0.993	0.925	1.020
ρ_{min}, ρ_{max} (e Å^{-3})	−0.22, 0.33	−0.32, 0.33	−0.28, 0.25	−0.21, 0.23

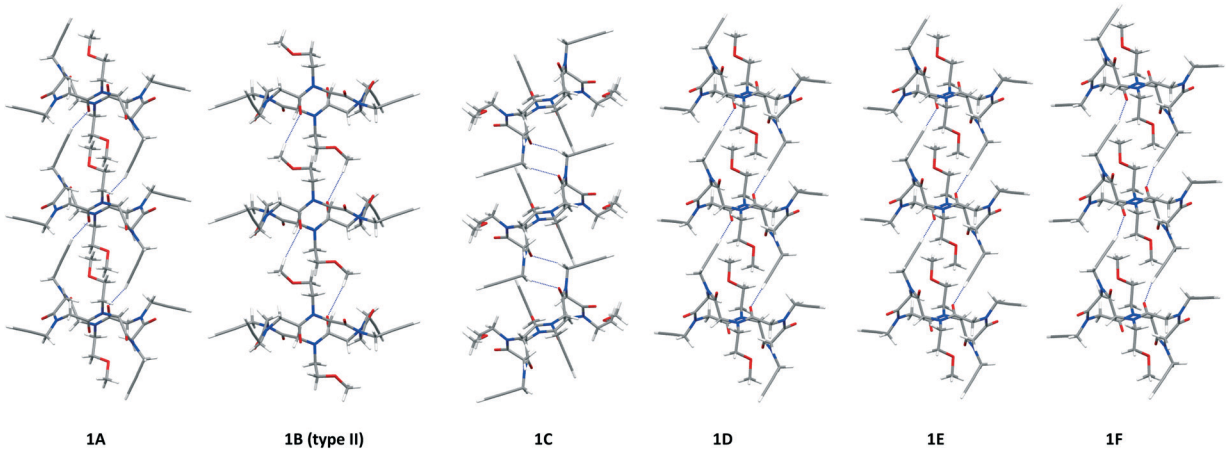

Fig. 1 Arrangement of cyclopeptoid molecules along the shortest crystallographic axis in the crystal forms **1A**, **1B** type II molecules, **1C**, **1D**, **1E** and **1F**. C═O···H–C hydrogen bonds are depicted as dotted lines. Atom types: C grey, N blue, O red, H white.

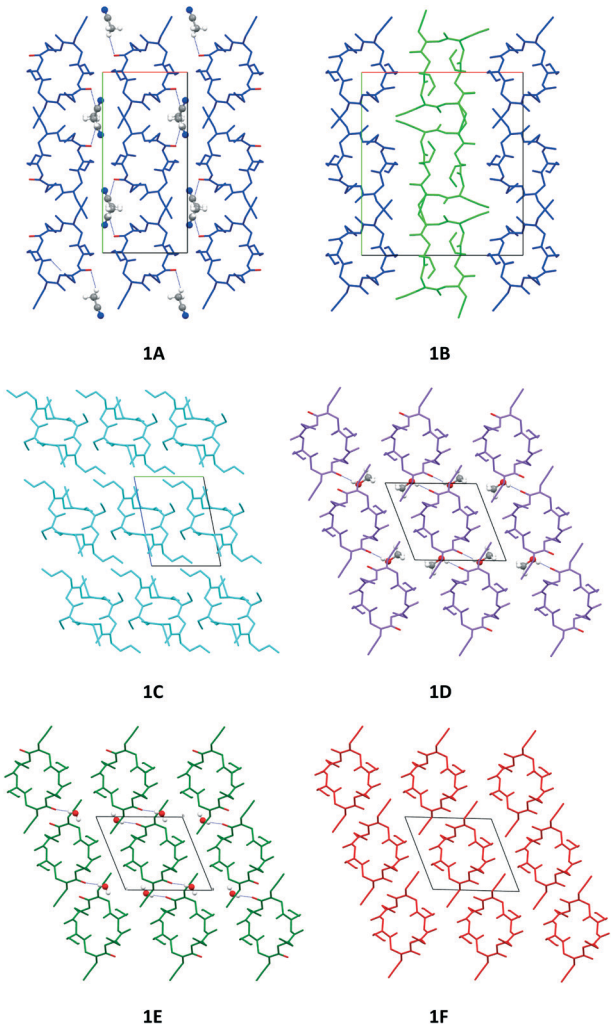

Fig. 2 Crystal packing of the crystal forms **1A**, **1B** (type I molecules in blue; type II molecules in green), **1C**, **1D**, **1E** and **1F** viewed along the shortest crystallographic axis. Host binding sites are highlighted in red. Guest molecules are depicted as ball and stick models. Hydrogen atoms are visualized only for guest molecules.

Indeed, acetonitrile molecules in form **1A** occupy channels (with a volume of 196.2 Å^3, Fig. 2 and 3a) and bind to the *cis* carbonyl oxygen atoms O3 (CO···HC 2.65 Å, CO···HO 157°, Fig. S7a, ESI†). Notably, the assembly of columns in **1D** and **1A** is different, as the intercolumnar interactions in **1D** and **1A** are mediated by the guest molecules, which are attached to different sides of the columns (Fig. 2). In **1D**, the columns pack in an approximately hexagonal arrangement, while in **1A** the columns shifted by one half along the shortest cell axis.

Thermal analyses were carried out for both crystal forms **1C** and **1D**. In the case of **1C**, DSC shows that the sample is stable up to 190 °C, and decomposes thereafter (Fig. S10, ESI†).

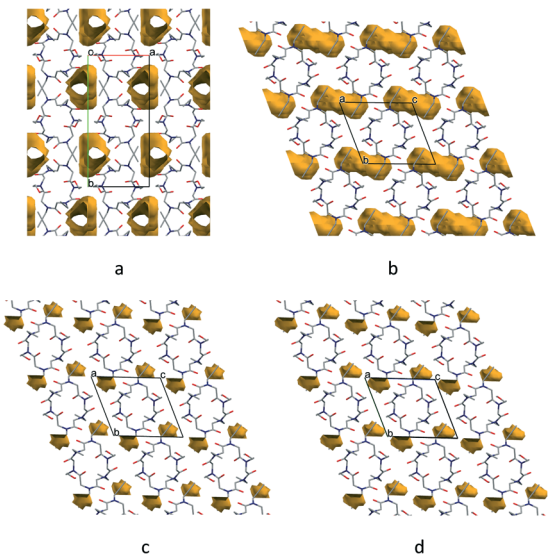

Fig. 3 Contact surfaces (yellow) in the crystal structures of **1** (probe radius: 1.2 Å). a) Form **1A**: channels (V = 196.2 Å^3 per unit cell) parallel to the c axis; b) form **1D**: cavities (V = 84.4 Å^3) stacked along the c axis; c) form **1E**: cavities (V = 11.9 Å^3) stacked along the c axis; d) form **1F**: cavities stacked along the c axis (V = 14.6 Å^3).

For **1D**, DSC and TGA reveal that desolvation occurs in one step over a wide temperature range from 30 °C to 90 °C (Fig. S11 and S12, ESI†). DSC also shows two closely occurring endothermic and exothermic events, starting at 184 °C and 215 °C, respectively. Finally, decomposition occurs at $T > 230$ °C (Fig. S11, ESI†).

The observed percentage weight loss of 8.2% from TGA corresponds to 1.7 molecules of methanol per cyclopeptoid molecule, which is in agreement with the value determined from the single crystal X-ray structure analysis.

It is noteworthy that a single crystal of form **1D**, exposed to air at room temperature for 30 minutes, is able to exchange the methanol molecules with water molecules (as shown by single crystal X-ray diffraction), resulting in the crystal form **1E**. Crystal form **1E** is isostructural with **1D** (Fig. 2).

The cyclopeptoid molecules in the two crystal forms overlap with a RMSD value of 0.1904 Å, and also in this case, the macrocycle possesses a crystallographic inversion centre. The water molecules in form **1E** occupy the cavities (with a volume of 11.9 $Å^3$, Fig. 3c) between the columns and are hydrogen bonded to the *cis* carbonyl oxygen atoms O2 (CO···HO distance 1.92 Å, CO···HO angle 167°). The carbonyl oxygen atoms O2 act again as H-bond binding sites (Fig. S7e, ESI†).

To test the crystal stability in the absence of guest molecules, an *in situ* variable temperature single crystal X-ray diffraction experiment was performed (see the ESI† for details). A fresh crystal of **1D** was flash cooled in liquid nitrogen and analyzed at 100 K to confirm the presence of methanol molecules; it was then heated using a hot air blower, measured at 323 K, 368 K and 393 K and cooled back to 100 K. The structure determinations revealed that methanol molecules left the crystal at 323 K to give rise to the isostructural apohost **1F**. The cyclopeptoid molecules in the **1E** and **1F** crystal forms overlap within a RMSD value of 0.0705 Å, and also in this case, the macrocycle possesses a crystallographic inversion centre.

Importantly, the columnar architecture remains intact and voids the form (with a volume of 14.6 $Å^3$, Fig. 3d), showing the robustness of the framework upon solvent removal. Form **1F** remains stable in a nitrogen atmosphere from 100 K to 393 K.

Upon exposing to environmental humidity, the apohost **1F** results in form **1E**, meaning that the cavities are accessible to incoming and outgoing guest molecules.

Form **1F** has a lower packing coefficient (0.706) than the solvated crystal forms **1D** (0.766), **1E** (0.758) and **1A** (0.769). In **1C**, the packing coefficient is 0.724, indicating that the host–guest interactions in **1D** and **1E** favour a more efficient packing arrangement.

We also verified the reversibility of the exchange process between water and methanol molecules by an *in situ* single crystal XRD experiment, exposing a crystal of **1E** to methanol vapours in a capillary (see the ESI†). Structural analysis confirmed the transformation to form **1D**. Notably, the cavities contract considerably when they are occupied by water molecules (11.9 $Å^3$) instead of methanol molecules (84.4 $Å^3$). However, the volume of the cavities (14.6 $Å^3$) in the empty form **1F** does not change significantly with respect to the hydrate form **1E**.

In conclusion, the conformational flexibility of compound **1** is crucial to the observed solvatomorphism. The crystallization solvents are able to favour one conformation over the other, leading to either a one-dimensional columnar (**1A** and **1D**) or a two-dimensional layered assembly of cyclopeptoid molecules (**1C**). Once the columns are formed, they may assemble in different ways, and the interaction with the guest molecules such as acetonitrile or methanol drives the final assembly in the solid state, leading to a different sorption behaviour.

Indeed, compound **1** exhibits two different possible guest release and uptake mechanisms according to the exhibited crystal form:

- in **1A**, the host framework releases the guest molecules, yielding the non-isostructural apohost **1B**, which in turn adsorbs the incoming guest molecules and transforms back to **1A**;[11]

- in **1D** and **1E**, the host framework releases the guest molecules to give a zeolite-like isostructural apohost **1F**, with stable cavities open to incoming and outgoing guest molecules.

Finally, compound **1** represents a paradigmatic example of how conformational changes are induced by the external environment, leading to different aggregation modes with divergent properties, paving the way for the understanding of a similar behaviour in more complex systems such as polypeptides.

Conflicts of interest

There are no conflicts of interest to declare.

Acknowledgements

The research leading to these results has received funding from the People Programme (Marie Curie Actions) of the European Union's Seventh Framework Programme FP7 (2007-2013) under REA grant agreement no. PIRSES-GA-2012-319011. Funding from the University of Salerno (FARB) and COST Action CM1402 Crystallize are also acknowledged. We are grateful to Prof. R. Zanasi (Univ. of Salerno) for valuable discussions and to Centro di Cristallografia Strutturale (Univ. of Florence) for the access to X-ray facilities.

Notes and references

1 A. Gavezzotti, *Molecular aggregation, structure analysis and molecular simulation of crystals and liquids*, Oxford University Press, Oxford, 2nd edn, 2007.
2 J. W. Mullin, *Crystallization*, Butterworth-Heinemann, Oxford, 4th edn, 2001.
3 E. D. Bøjesen and B. B. Iversen, *CrystEngComm*, 2016, **18**, 8332–8353.
4 M. Zobel, R. B. Neder and S. A. J. Kimber, *Science*, 2015, **347**, 292–294.

5 L. R. Nassimbeni, *Acc. Chem. Res.*, 2003, **36**, 631–637.
6 A. J. Cruz-Cabeza and J. Bernstein, *Chem. Rev.*, 2014, **114**, 2170–2191.
7 For recent reviews on peptoids see: (*a*) N. Gangloff, J. Ulbricht, T. Lorson, H. Schlaad and R. Luxenhofer, *Chem. Rev.*, 2016, **116**, 1753–1802; (*b*) J. Sun and R. N. Zuckermann, *ACS Nano*, 2013, **7**, 4715–4732; (*c*) I. Izzo, C. De Cola and F. De Riccardis, *Heterocycles*, 2011, **82**, 981–1006; (*d*) A. S. Culf and R. J. Ouellette, *Molecules*, 2010, **15**, 5282–5335.
8 C. Tedesco, L. Erra, I. Izzo and F. De Riccardis, *CrystEngComm*, 2014, **16**, 3667–3687.
9 C. Tedesco, A. Meli, E. Macedi, V. Iuliano, A. G. Ricciardulli, F. De Riccardis, G. Vaughan, V. J. Smith, L. J. Barbour and I. Izzo, *CrystEngComm*, 2016, **18**, 8838–8848.
10 (*a*) C. Tedesco, E. Macedi, A. Meli, G. Pierri, G. Della Sala, C. Drathen, A. N. Fitch, G. B. M. Vaughan, I. Izzo and F. De Riccardis, *Acta Crystallogr., Sect. B: Struct. Sci., Cryst. Eng. Mater.*, 2017, **73**, 399–412; (*b*) R. Schettini, F. De Riccardis, G. Della Sala and I. Izzo, *J. Org. Chem.*, 2016, **81**, 2494–2505; (*c*) C. De Cola, G. Fiorillo, A. Meli, S. Aime, E. Gianolio, I. Izzo and F. De Riccardis, *Org. Biomol. Chem.*, 2014, **21**, 424–431; (*d*) I. Izzo, G. Ianniello, C. De Cola, B. Nardone, L. Erra, G. Vaughan, C. Tedesco and F. De Riccardis, *Org. Lett.*, 2013, **15**, 598–601; (*e*) N. Maulucci, I. Izzo, G. Bifulco, A. Aliberti, C. De Cola, D. Comegna, C. Gaeta, A. Napolitano, C. Pizza, C. Tedesco, D. Flot and F. De Riccardis, *Chem. Commun.*, 2008, 3927–3929.
11 A. Meli, E. Macedi, F. De Riccardis, V. J. Smith, L. J. Barbour, I. Izzo and C. Tedesco, *Angew. Chem., Int. Ed.*, 2016, **55**, 4679–4682.
12 Peptoid backbones of **1C** and **1D** overlap within a RMSD value of 0.062 Å (Fig. S4, ESI†). In both cases, the macrocycle has an approximately rectangular shape (Fig. S5, ESI†). The backbone conformation could mimic a β-turn structure as reported by: (*a*) B. Yoo, S. B. Y. Shin, M. L. Huang and K. Kirshenbaum, *Chem. – Eur. J.*, 2010, **16**, 5528–5537; (*b*) S. B. Y. Shin, B. Yoo, L. J. Todaro and K. Kirshenbaum, *J. Am. Chem. Soc.*, 2007, **129**, 3218–3225.
13 M. J. Frisch, *et al.*, *Gaussian 09, revision A.1*, Gaussian, Inc., Wallingford, CT, 2009.
14 (*a*) M. A. Spackman and D. Jayatilaka, *CrystEngComm*, 2009, **11**, 19–32; (*b*) J. J. McKinnon, M. A. Spackman and A. S. Mitchell, *Acta Crystallogr., Sect. B: Struct. Sci.*, 2004, **60**, 627–668; (*c*) M. A. Spackman and J. J. McKinnon, *CrystEngComm*, 2002, **4**, 378–392.
15 (*a*) A. Gavezzotti, *New J. Chem.*, 2011, **35**, 1360–1368; (*b*) A. Gavezzotti, *J. Phys. Chem. B*, 2003, **107**, 2344–2353; (*c*) A. Gavezzotti, *J. Phys. Chem. B*, 2002, **106**, 4145–4154.
16 The cyclopeptoid molecules in **1A** and **1D** overlap within a RMSD of 0.331 Å.
17 C. F. Macrae, I. J. Bruno, J. A. Chisholm, P. R. Edgington, P. McCabe, E. Pidcock, L. Rodriguez-Monge, R. Taylor, J. van de Streek and P. A. Wood, *J. Appl. Crystallogr.*, 2008, **41**, 466–470.

